Inorg. Chem. **1989**, *28*, 4051-4053

Contribution from the Department of Chemistry
and Molecular Structure Center,
Indiana University, Bloomington, Indiana 47405

Structure, Dynamics, and Comparative Stability of a Mixed-Ligand Compound of Tin(II)

Michael J. McGeary, Kirsten Folting, and Kenneth G. Caulton*

Received March 30, 1989

The bulky group 14 metal(II) amide compounds $\mathrm{M[N(SiMe_3)_2]_2}$ (M = Ge, Sn, Pb) have extensive transition-metal coordination chemistry both as neutral, terminal ligands (ylene complexes) and as four-coordinate ligands bridging two transition-metal centers. For a thorough review of this subject, consult ref 1.

Heterometallic tin/copper complexes bearing ligands easily hydrolyzed to form oxo groups are currently of interest because of their relevance to potential low-temperature syntheses of superconducting materials.[2] An attractive entry into such tin/copper complexes was envisioned as the combination of $\mathrm{Sn[N(SiMe_3)_2]_2}$ with $\mathrm{[Cu(O^tBu)]_4}$ in the expectation of forming a copper(I) stannylene complex such as that depicted by I. This expectation was not fulfilled; instead, products resulting from ligand redistribution were formed as described below.

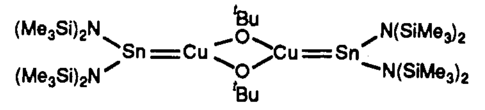

I

Results and Discussion

The reaction of $\mathrm{[Cu(O^tBu)]_4}$ with $\mathrm{Sn[N(SiMe_3)_2]_2}$ in hexane, followed by concentration to the point of crystallization, yielded a pure product identified by spectroscopy and X-ray diffraction as $\mathrm{[Sn(N(SiMe_3)_2)(\mu\text{-}O^tBu)]_2}$ (**1**; eq 1). The overall 1:1 ratio

$$0.25\mathrm{[Cu(O^tBu)]_4} + \mathrm{Sn[N(SiMe_3)_2]_2} \rightarrow 0.5\mathrm{[Sn(N(SiMe_3)_2)(\mu\text{-}O^tBu)]_2} + \ldots \quad (1)$$

of $\mathrm{-O^tBu}$ and $\mathrm{-N(SiMe_3)_2}$ groups was established by integration of the ^{1}H NMR signals, but the trimethylsilyl region of the spectrum exhibited unanticipated complexity: two singlets of identical intensity. A complementary pattern of resonances for the $\mathrm{-O^tBu}$ and $\mathrm{-N(SiMe_3)_2}$ carbons was observed in the ^{13}C NMR spectrum.

The X-ray structure determination revealed a centrosymmetric dimer devoid of copper with two bridging $\mathrm{-O^tBu}$ groups, two terminal, mutually trans $\mathrm{-N(SiMe_3)_2}$ groups, and pyramidally configured Sn(II) cores (Figures 1 and 2). The $\mathrm{Sn_2O_2}$ rhombus has identical Sn–O bond lengths, and the oxygen centers are planar (angles at O sum to 359.9°), as are the nitrogen centers (angles at N sum to 359.7°). Obtuse Sn–O–Sn′ angles together with the large Sn–Sn′ separation (3.510 (1) Å) indicate no attractive interactions between the metal atoms. Similar structures have been found for other ligand-bridged tin(II) dimers, for example: $\mathrm{[Sn(NMe_2)(\mu\text{-}NMe_2)]_2}$,[3a] $\mathrm{[Sn(Cl)(\mu\text{-}O^tBu)]_2}$,[3b] and $\mathrm{[Sn(O^tBu)(\mu\text{-}O^tBu)]_2}$ (gas electron diffraction).[3c]

The rotational conformation about the Sn–N bonds places the $\mathrm{-SiMe_3}$ groups in inequivalent environments: one over the $\mathrm{Sn_2O_2}$ rhomb and the other directed toward a tin lone pair. The observation of two $\mathrm{-SiMe_3}$ ^{1}H NMR resonances carries two implications: (i) that Sn–N rotation is slow on the NMR time scale and (ii) that scission of the Sn–O bridges yielding monomeric $\mathrm{Sn(O^tBu)[N(SiMe_3)_2]}$ is also slow on the NMR time scale. We note here that in the related dimer $\mathrm{[Sn(O^tBu)(\mu\text{-}O^tBu)]_2}$ terminal and bridging $\mathrm{-O^tBu}$ groups rapidly interchange, presumably via dissociation to $\mathrm{Sn(O^tBu)_2}$ monomers.[4] The importance of interligand steric factors is evident in the hindered rotation of the $\mathrm{-N(SiMe_3)_2}$ group, where one $\mathrm{-SiMe_3}$ arm of each amide ligand is trapped between two $\mathrm{-O^tBu}$ groups as depicted in the space-filling drawing (Figure 2). Evidence for site exchange between the inequivalent $\mathrm{-SiMe_3}$ groups at 25 °C was provided by two-dimensional NOESY ^{1}H NMR techniques, which revealed off-diagonal peaks connecting the $\mathrm{-SiMe_3}$ resonances at 0.49 and 0.39 ppm. A cross peak between the 1.37 ppm $\mathrm{-O^tBu}$ signal and the 0.39 ppm $\mathrm{-SiMe_3}$ signal was detected. This was attributed to through-space nuclear Overhauser relaxation and established the physical proximity of these methyl groups, allowing assignment of the 0.39 ppm resonance to the $\mathrm{-SiMe_3}$ group positioned over the $\mathrm{Sn_2O_2}$ rhomb. An additional cross peak of very low intensity was detected between the 0.49 ppm $\mathrm{-SiMe_3}$ signal and the $\mathrm{-O^tBu}$ signal and was ascribed to through-space NOE relaxation *after* $\mathrm{-SiMe_3}$ site exchange.

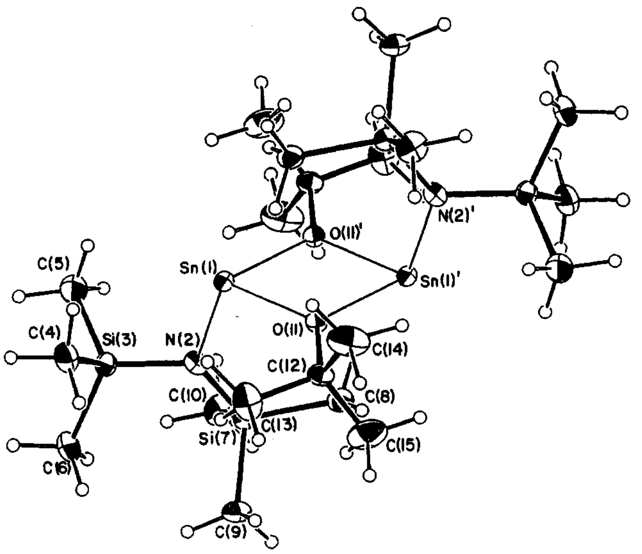

Figure 1. ORTEP drawing of $\mathrm{[Sn(N(SiMe_3)_2)(\mu\text{-}O^tBu)]_2}$ showing the two inequivalent $\mathrm{SiMe_3}$ groups on each nitrogen. Primed atoms are related to those unprimed by a crystallographic center of inversion.

The selectivity for the mixed-ligand tin compound in the $\mathrm{[Cu(O^tBu)]_4/Sn[N(SiMe_3)_2]_2}$ metathesis reaction was unanticipated. Indeed, the ^{1}H NMR spectra of solutions containing $\mathrm{[Sn(N(SiMe_3)_2)(\mu\text{-}O^tBu)]_2}$ exhibited additional weak resonances in the $\mathrm{-O^tBu}$ and $\mathrm{-SiMe_3}$ regions. Certain of these (1.44, 1.42, 0.45, 0.43, 0.42, 0.38, 0.31, 0.28, 0.26 ppm) gain intensity on heating to 67 °C in $\mathrm{C_6D_6}$. The intensities of these other resonances declined somewhat on prompt recooling, but the original intensity ratios were not accurately reestablished until several hours later. Since some of these weak resonances match those of $\mathrm{Sn[N(SiMe_3)_2]_2}$ (s, 0.28 ppm) and $\mathrm{[Sn(O^tBu)(\mu\text{-}O^tBu)]_2}$ (s, 1.44 ppm), a temperature-dependent equilibrium involving at least the species outlined in eq 2 is suggested with compound **1** predominating at

$$2\underset{\mathbf{1}}{\mathrm{[Sn(N(SiMe_3)_2)(\mu\text{-}O^tBu)]_2}} \rightleftarrows 2\mathrm{Sn[N(SiMe_3)_2]_2} + \mathrm{[Sn(\mu\text{-}O^tBu)(O^tBu)]_2} \quad (2)$$

25 °C. Consistent with this view, $\mathrm{[Sn(N(SiMe_3)_2)(\mu\text{-}O^tBu)]_2}$ was isolated from the reaction of $\mathrm{Sn[N(SiMe_3)_2]_2}$ with $\mathrm{[Sn(O^tBu)(\mu\text{-}O^tBu)]_2}$. Since entropy favors the right side of eq 2, there is a clearly defined enthalpic preference for the mixed-ligand dimer **1** over homoleptic $\mathrm{[Sn(O^tBu)(\mu\text{-}O^tBu)]_2}$ and $\mathrm{Sn[N(SiMe_3)_2]_2}$. The finding that $\mathrm{-O^tBu}$, not $\mathrm{-N(SiMe_3)_2}$, bridges in **1**, together with

---

(1) Lappert, M. F. *Silicon, Germanium, Tin Lead Compd.* **1986**, *9*, 129.
(2) Hubert-Pfalzgraf, L. G. *New J. Chem.* **1987**, *11*, 663.
(3) (a) Olmstead, M. M.; Power, P. P. *Inorg. Chem.* **1984**, *23*, 413. (b) Zybill, C.; Müller, G. *Z. Naturforsch.* **1988**, *43B*, 45. (c) Fjeldberg, T.; Hitchcock, P. B.; Lappert, M. F.; Smith, S. J.; Thorne, A. J. *J. Chem. Soc., Chem. Commun.* **1985**, 939.
(4) Veith, M.; Töllner, F. *J. Organomet. Chem.* **1983**, *246*, 219.

0020-1669/89/1328-4051$01.50/0

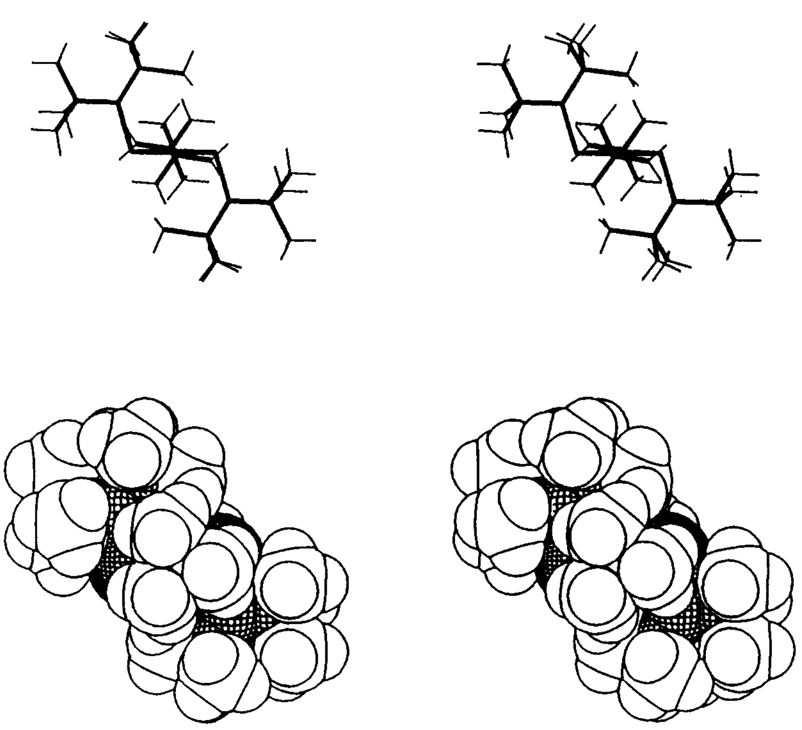

Figure 2. Stereo stick-figure (top) and space-filling models (bottom) of $[Sn(N(SiMe_3)_2)(\mu\text{-}O^tBu)]_2$.

the monomeric nature of $Sn[N(SiMe_3)_2]_2$, establishes that $-O^tBu$ is superior to $-N(SiMe_3)_2$ as a bridging group for tin(II). Similar temperature-dependent equilibria have been postulated for $[Sn(Cl)(\mu\text{-}O^tBu)]_2$ on the basis of NMR studies.[3b] Interestingly, Lappert and co-workers have found that a related lead(II) dimer, $[Pb(N(SiMe_3)_2)(\mu\text{-}SC(SiMe_3)_3)]_2$, irreversibly redistributes ligands, forming $Pb[N(SiMe_3)_2]_2$ and $[Pb(SC(SiMe_3)_3)(\mu\text{-}SC(SiMe_3)_3)]_2$ at 20 °C in hexane or benzene.[5]

In conclusion, while the methods explored here yielded no isolable mixed-metal Sn/Cu compounds, the intermediacy of such a derivative(s) is implicit in the synthetic reaction (eq 1). Our results do suggest that ligand metathesis can be a complicating factor in building Cu(I)–alkoxide–main-group-metal multimetallic systems. Future efforts toward this synthetic goal will probably be facilitated by focusing on reactions between metal reagents with identical ligands so that metathesis becomes degenerate.

Experimental Section

Materials and Methods. All manipulations were performed by using standard Schlenk techniques either in vacuo or under an atmosphere of nitrogen. Hexane and pentane solvents were dried over potassium benzophenone ketyl, distilled under nitrogen, and subjected to three freeze–evacuate–thaw cycles prior to use. Deuterated solvents, C_6D_6 and toluene-d_8, were dried similarly and distilled in vacuo. $Sn[N(SiMe_3)_2]_2$[6a] and $[Cu(O^tBu)]_4$[6b] were prepared according to literature procedures. $[Sn(O^tBu)(\mu\text{-}O^tBu)]_2$[3c,4] was prepared from $Sn[N(SiMe_3)_2]_2$ and 2 equiv of *tert*-butyl alcohol and purified by sublimation prior to use. Yields reported here have not been optimized.

Physical Measurements. Infrared spectra were recorded as Nujol mulls with a Perkin-Elmer 283 spectrophotometer. Hydrogen-1 and carbon-13 NMR spectra were recorded on a Bruker 500 instrument (^1H and 500 MHz and ^{13}C at 125.7 MHz) and referenced to Me_4Si. Tin-119 NMR spectra were recorded on a Nicolet 360 instrument (^{119}Sn at 134.2 MHz) and referenced to Me_4Sn.

Syntheses. Method i. A 100-mL Schlenk flask was charged with 0.08 g (0.15 mmol) of $[Cu(O^tBu)]_4$ and 20 mL of hexane. The resultant pale yellow suspension was chilled to 0 °C, whereupon 0.25 g (0.57 mmol) of $Sn[N(SiMe_3)_2]_2$ was added. The mixture was stirred 5 h, during which time it was permitted to gradually attain room temperature. The mixture was then filtered through a plug of Celite, and the volume of the nearly colorless filtrate was reduced to 5 mL in vacuo. When the solution stood at −20 °C for 12 h, ivory crystals precipitated. The crystals were washed with cold (−80 °C) pentane and dried in vacuo; yield 60%.

Table I. Crystallographic Data for $[Sn(N(SiMe_3)_2)(\mu\text{-}O^tBu)]_2$

chem formula	$C_{20}H_{54}N_2O_2Si_4Sn_2$	space group	$P2_1/a$
a, Å	10.310 (2)	T, °C	−141
b, Å	14.249 (2)	λ, Å	0.71069
c, Å	11.316 (2)	ρ_{calcd}, g cm^{-3}	1.422
β, deg	98.20 (1)	μ(Mo Kα), cm^{-1}	16.8
V, Å^3	1645.36	R	0.0337
Z	2	R_w	0.0320
fw	704.38		

Method ii. A 100-mL Schlenk flask was charged with 0.13 g (0.25 mmol) of $[Sn(O^tBu)(\mu\text{-}O^tBu)]_2$ and 0.22 g (0.50 mmol) of $Sn[N(SiMe_3)_2]_2$. Hexane (20 mL) was added. The mixture was stirred 3 h, followed by reduction of the solvent volume to 2 mL. When the solution stood in the freezer overnight, ivory crystals precipitated. These were isolated as outlined above; yield 70%. IR (Nujol): ν(C–O) 1255, 1248 cm^{-1}. ^1H NMR (toluene-d_8): δ 1.37 (s, 18 H, $OC(CH_3)_3$); 0.49 (s, 18 H, $SiMe_3$); 0.39 (s, 18 H, $SiMe_3$). ^{13}C NMR (C_6D_6): δ 76.1 ($-OC(CH_3)_3$); 33.1 ($-OC(CH_3)_3$); 7.3, 6.7 ($-Si(CH_3)_3$). ^{119}Sn NMR (C_6D_6): δ 41.8 (vbr). MS (CI, NH_3; m/z (assignment)): 677 ($M^+ - 2CH_3$).

X-ray Diffraction Study of $Sn_2(O^tBu)_2[N(SiMe_3)_2]_2$. A small, almost equidimensional crystal was mounted with use of inert-atmosphere handling techniques. The crystal was transferred to the goniostat, where it was cooled to −141 °C for characterization and data collection.[7] A systematic search of a limited hemisphere of reciprocal space yielded a set of reflections that exhibited monoclinic symmetry ($2/m$). The systematic extinction of $0k0$ for $k = 2n + 1$ and of $h0l$ for $h = 2n + 1$ uniquely identified the space group as $P2_1/a$. Details of the data collection ($6° \leq 2\theta \leq 45°$) and refinement are given in Table I. The standard reflections showed no systematic trends. An examination of ψ scans indicated that no absorption correction was necessary. The structure was solved by locating the Sn atom by means of MULTAN. The non-hydrogen atoms were located in a difference Fourier phased by the Sn atom. The asymmetric unit contains half of a Sn dimer since the molecule possesses a crystallographic center of symmetry. All hydrogen atoms were located in a difference map following the initial refinement. The full-matrix least-squares refinement was completed by using anisotropic thermal parameters on all non-hydrogen atoms and isotropic thermal parameters on the hydrogen atoms. The final difference map was essentially featureless; the largest peak was 0.82 e/Å^3 in the vicinity

---

(5) Hitchcock, P. B.; Jasim, H. A.; Kelly, R. E.; Lappert, M. F. *J. Chem. Soc., Chem. Commun.* **1985**, 1776.

(6) (a) Harris, D. H.; Lappert, M. F. *J. Chem. Soc., Chem. Commun.* **1974**, 895. (b) Tsuda, T.; Hashimoto, T.; Saegusa, T. *J. Am. Chem. Soc.* **1972**, *94*, 658.

(7) For X-ray methods, see: Huffman, J. C.; Lewis, L. N.; Caulton, K. G. *Inorg. Chem.* **1980**, *19*, 2755.

Inorg. Chem. **1989**, *28*, 4053-4055

Table II. Fractional Coordinates[a] and Isotropic Thermal Parameters[b] for $[Sn(N(SiMe_3)_2)(\mu\text{-O}^tBu)]_2$

	x	y	z	$10B_{iso}$, Å^2
Sn(1)	4108.3 (4)	4187.3 (3)	9040.4 (3)	13
N(2)	3319 (4)	4946 (3)	7483 (4)	14
Si(3)	2355 (2)	4177 (1)	6539 (1)	16
C(4)	3227 (7)	3034 (5)	6412 (7)	24
C(5)	781 (8)	3922 (6)	7148 (7)	30
C(6)	1931 (8)	4577 (6)	4960 (6)	26
Si(7)	3367 (2)	6128 (1)	7121 (1)	15
C(8)	4224 (7)	6881 (5)	8332 (6)	21
C(9)	4255 (7)	6322 (5)	5804 (6)	22
C(10)	1678 (7)	6635 (6)	6778 (7)	26
O(11)	6021 (4)	4826 (3)	9517 (3)	14
C(12)	7186 (6)	4692 (4)	8936 (5)	17
C(13)	6808 (7)	4062 (7)	7854 (7)	34
C(14)	8214 (8)	4219 (7)	9810 (7)	36
C(15)	7647 (8)	5634 (6)	8536 (8)	36
H(1)	340 (7)	263 (5)	715 (7)	43 (7)
H(2)	265 (9)	260 (7)	587 (7)	62 (7)
H(3)	396 (8)	310 (5)	606 (7)	39 (7)
H(4)	46 (9)	445 (7)	733 (8)	55 (6)
H(5)	44 (10)	353 (8)	664 (9)	75 (6)
H(6)	109 (9)	357 (7)	791 (9)	68 (6)
H(7)	151 (8)	514 (7)	489 (7)	54 (6)
H(8)	276 (8)	464 (5)	461 (6)	34 (7)
H(9)	145 (9)	420 (6)	453 (7)	50 (6)
H(10)	510 (10)	673 (7)	849 (8)	67 (6)
H(11)	407 (8)	749 (7)	810 (7)	48 (7)
H(12)	385 (5)	690 (4)	902 (5)	15 (7)
H(13)	504 (10)	615 (7)	594 (8)	58 (7)
H(14)	374 (10)	615 (7)	511 (9)	70 (7)
H(15)	432 (7)	703 (6)	568 (6)	46 (7)
H(16)	177 (12)	721 (9)	661 (10)	99 (6)
H(17)	103 (11)	635 (9)	609 (10)	94 (6)
H(18)	111 (10)	658 (7)	724 (9)	70 (6)
H(19)	602 (10)	428 (7)	727 (8)	65 (6)
H(20)	760 (9)	403 (5)	757 (7)	48 (7)
H(21)	630 (10)	350 (7)	799 (8)	66 (6)
H(22)	801 (7)	354 (5)	998 (6)	32 (7)
H(23)	849 (10)	463 (7)	1046 (9)	75 (6)
H(24)	891 (8)	424 (5)	951 (7)	42 (6)
H(25)	842 (7)	556 (4)	812 (6)	26 (7)
H(26)	788 (13)	606 (9)	920 (11)	109 (5)
H(27)	702 (12)	588 (8)	811 (10)	87 (5)

[a] Fractional coordinates are ×10^4 for non-hydrogen atoms and ×10^3 for hydrogen atoms. B_{iso} values are ×10. [b] Isotropic values for those atoms refined anisotropically are calculated with use of the formula given by: Hamilton, W. C. *Acta Crystallogr.* **1959**, *12*, 609.

Table III. Selected Bond Distances (Å) and Angles (deg) for $[Sn(N(SiMe_3)_2)(\mu\text{-O}^tBu)]_2$

Sn(1)-Sn(1)′	3.5102 (9)	Si(7)-N(2)	1.736 (5)
Sn(1)-O(11)	2.168 (4)	Si(7)-C(8)	1.862 (7)
Sn(1)-O(11)′	2.173 (4)	Si(7)-C(9)	1.877 (7)
Sn(1)-N(2)	2.128 (5)	Si(7)-C(10)	1.874 (7)
Si(3)-N(2)	1.740 (5)	O(11)-C(12)	1.462 (7)
Si(3)-C(4)	1.876 (7)	C(12)-C(13)	1.523 (10)
Si(3)-C(5)	1.886 (7)	C(12)-C(14)	1.502 (10)
Si(3)-C(6)	1.868 (7)	C(12)-C(15)	1.515 (10)
O(11)-Sn(1)-O(11)′	72.10 (15)	C(9)-Si(7)-C(10)	108.8 (4)
O(11)-Sn(1)N(2)	102.67 (17)	Sn(1)-O(11)-Sn(1)′	107.90 (15)
O(11)′-Sn(1)-N(2)	103.69 (17)	Sn(1)-O(11)-C(12)	127.6 (3)
N(2)-Si(3)-C(4)	110.8 (3)	Sn(1)′-O(11)-C(12)	124.4 (3)
N(2)-Si(3)-C(5)	110.1 (3)	Sn(1)-N(2)-Si(3)	107.82 (25)
N(2)-Si(3)-C(6)	115.5 (3)	Sn(1)-N(2)-Si(7)	131.91 (26)
C(4)-Si(3)-C(5)	107.9 (4)	Si(3)-N(2)-Si(7)	119.95 (27)
C(4)-Si(3)-C(6)	103.9 (4)	O(11)-C(12)-C(13)	107.8 (5)
C(5)-Si(3)-C(6)	108.2 (4)	O(11)-C(12)-C(14)	108.1 (5)
N(2)-Si(7)-C(8)	114.33 (28)	O(11)-C(12)-C(15)	109.4 (5)
N(2)-Si(7)-C(9)	111.3 (3)	C(13)-C(12)-C(14)	109.9 (6)
N(2)-Si(7)-C(10)	111.5 (3)	C(13)-C(12)-C(15)	109.7 (6)
C(8)-Si(7)-C(9)	105.4 (3)	C(14)-C(12)-C(15)	111.8 (7)
C(8)-Si(7)-C(10)	105.0 (4)		

of the Sn atom. The results of the structure determination are given in Tables II and III and Figures 1 and 2. Refined C-H distances range from 0.82 (11) to 1.03 (12) Å.

Acknowledgment. This work was supported by the Department of Energy. We thank Scott Horn for skilled technical assistance.

Supplementary Material Available: Full crystallographic details (Table S1) and anisotropic thermal parameters (Table S2) (2 pages); observed and calculated structure factors (Table S3) (5 pages). Ordering information is given on any current masthead page.

Contribution from the Department of Chemistry,
Department of Chemical Engineering, and Center
for Micro-Engineered Ceramics, University of
New Mexico, Albuquerque, New Mexico 87131

Synthesis of Boron Nitride Ceramics from 2,4,6-Triaminoborazine

Chaitanya K. Narula,[†,§] Riley Schaeffer,[†] Ahbaya Datye,[‡]
and Robert T. Paine[*,†]

Received March 15, 1989

The hexagonal crystalline modification of boron nitride is often prepared by pyrolysis of simple starting materials, such as boric acid and urea, or by plasma and chemical vapor deposition techniques from mixtures of ammonia and diborane(6) or boron trihalides.[1] Even though these syntheses are useful, Wynne and Rice[2] have pointed out that increasingly sophisticated applications for boron nitride demand the development of new approaches for forming and processing this ceramic. In response, several groups have sought molecular- and polymer-based syntheses that may offer advantages for forming BN fibers, films, and composites.[3] For example, Rice and co-workers[4] and Paciorek and co-workers[5] have described the pyrolysis chemistry of several substituted borazenes, $[RNBR']_3$. At modest temperatures, several borazenes were found to oligomerize, and at higher pyrolysis temperatures, ceramic products were produced. Sneddon and co-workers[6] have observed that, in the presence of ammonia, conversion of commercial $Me_2S\cdot B(H)Br_2$, *B*-alkenylpentaborane, and *B*-alkenylborazene to polymeric ceramic precursors occurs. Pyrolysis of these precursors provide h-BN. Further, Rees and Seyferth[7] have found that oligomeric $[B_{10}H_{12}(\text{diamine})]_n$ reagents produce h-BN when pyrolyzed in NH_3. Indeed, several of these precursors may be used to produce fibers and films.[5-7]

In our group, we have previously described cross-linking reactions of *B*-chloroborazenes with hexamethyldisilazane.[8] Subsequent pyrolyses of the oligomers produce pure h-BN or carbon-contaminated boron nitride, depending upon the monomer employed and the pyrolysis conditions. We report here alternative deamination chemistry of a readily available borazene, $[HNB(NMe_2)]_3$, and conversion of the resulting solid polymers to h-BN.

Experimental Section

General Information. Standard inert-atmosphere techniques were used for the preparation and manipulation of all reagents. Solvents were carefully dried with appropriate drying agents and distilled under dry nitrogen. Infrared spectra were recorded on a Nicolet FT-IR Model 6000 spectrometer, and NMR spectra were recorded on Varian FT-80A and JEOL GSX-400 spectrometers. Spectral standards were $(CH_3)_4Si$ (^1H) and $BF_3\cdot O(C_2H_5)_2$ (^{11}B). $[(CH_3)_2NBNH]_3$ was prepared as described in the literature.[9] Thermal gravimetric analyses were performed on a Du Pont Model 1090 TGA instrument. EDS analyses were performed by using a Tracor Northern Model 5500 system with a high take off detector. The sample tilt was 0° during X-ray analysis. The transmission electron microscope used was a JEOL JEM-2000 FX instrument operated at 200 kV. The point resolution was ~0.3 mm. The powder surface area and density were determined by the BET method and helium pycnometry, respectively.

[†] Department of Chemistry.

[‡] Department of Chemical Engineering.

[§] Present address: Chemistry Department, Ford Motor Co., Dearborn, MI 48121-2053.

0020-1669/89/1328-4053$01.50/0